

New method to detect a heavy top quark at the Fermilab Tevatron

C.-P. Yuan

High Energy Physics Division, Argonne National Laboratory, Argonne, Illinois 60439

(Received 15 May 1989)

We present a new method to detect a heavy top quark with mass ~ 180 GeV at the upgraded Fermilab Tevatron ($\sqrt{S} = 2$ TeV and integrated luminosity 100 pb^{-1}) and the Superconducting Super Collider (SSC) via the W -gluon fusion process. We show that an almost perfect efficiency for the “kinematic b tagging” can be achieved due to the characteristic features of the transverse momentum P_T and rapidity Y distributions of the spectator quark which emitted the virtual W . Hence, we can reconstruct the invariant mass M^{evb} and see a sharp peak within a 5-GeV-wide bin of the M^{evb} distribution. We conclude that more than one year of running is needed to detect a 180-GeV top quark at the upgraded Tevatron via the W -gluon fusion process. Its detection becomes easier at the SSC due to a larger event rate.

I. INTRODUCTION

The yet to be found top quark is required in many aspects, either experimentally¹ or theoretically.² Recently, the Collider Detector at Fermilab (CDF) Collaboration³ has set a lower bound on the top-quark mass of about 78 GeV. Any value in the range of $78 \leq m_t \leq 200$ GeV may, therefore, be allowed at present.⁴ The Fermilab Tevatron will permit a top-quark search up to about 100 GeV in the near future, and possibly up to 150 GeV for an upgraded Tevatron ($\sqrt{S} = 2$ TeV and integrated luminosity 100 pb^{-1}) by detecting the dilepton, or lepton + jet production of the $t\bar{t}$ final state. Extensive references may be found in Ref. 5 for the signatures of the top quark if $m_t \leq M_W$. For $m_t \geq M_W$, the signatures of the top quark via the $p\bar{p} \rightarrow t\bar{t}X \rightarrow b\bar{b}W^+W^-X$ process have also been studied by various groups.⁶

In this paper we will study the production of a heavy quark at the upgraded Tevatron and the Superconducting Super Collider (SSC) via the W -gluon fusion process, shown in Fig. 1. The heavy quark can be a top quark or a sequential fourth-generation quark. We pay special attention to the characteristic features of the transverse momentum P_T and the rapidity Y distributions of the spectator quark which emitted the virtual W . From these unique features we develop a “kinematic b -tagging” algorithm for this process: its efficiency is almost 100%.

Notice that the “kinematic b -tagging” method introduced here is based on the unique kinematic features of the W -gluon fusion process. It is *not* the usual b tagging achieved by tagging on the muon via $b \rightarrow \mu^- \bar{\nu} X$ or using a fine vertex vector.⁷

We also introduced an algorithm⁸ to find the longitudinal momentum of the neutrino coming from the decay of the real W produced by the decay of the top quark. We can then reconstruct the top-quark mass and see a sharp peak within a 5-GeV-wide bin of the invariant mass M^{evb} . As an example, we choose a 180-GeV top quark to perform a Monte Carlo study at both the upgraded

Tevatron and SSC, and we conclude that the W -gluon fusion mechanism is indeed useful in detecting such a top quark. The same conclusion should hold for any top quark with $m_t > M_W$. The relative event rate of the W -gluon fusion mechanism versus the $t\bar{t}$ production mechanism grows as the top-quark mass increases. Hence the W -gluon fusion mechanism becomes increasingly important as the top-quark mass gets heavier, provided there are enough signal events retained to yield a reasonable signal-to-background ratio in the analysis. For instance, this production mechanism will work better for detecting a 140-GeV top quark than a 90-GeV top quark.

The remainder of this paper is organized as follows. In Sec. II we review some results of top-quark detection via the QCD processes qq or $gg \rightarrow t\bar{t}$. In Sec. III we discuss how to detect a heavy quark via the W -gluon fusion process and compare this strategy with the above one, i.e., via the pure QCD processes. In Sec. IV we present a Monte Carlo study for the detection of a 180-GeV top

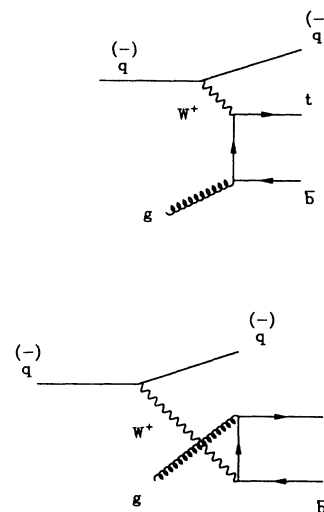


FIG 1. Feynman diagrams for the W -gluon fusion process.

quark at the upgraded Tevatron. The $W+3$ jet background will also be studied using a parton-level Monte Carlo program written by Dieter Zeppenfeld, W. Long, T. Han, and Dorothea Zeppenfeld.⁹ A separate study using the parton-level Monte Carlo program PAPAGENO (Ref. 10) is also given in the Appendix for comparison. Section V. is devoted to the detection of the same top quark at the SSC. We conclude our study in Sec. VI.

II. HADRONIC $t\bar{t}$ PRODUCTION

The production of a heavy quark in hadronic collisions arises from the standard lowest-order [$O(\alpha_s^2)$] QCD subprocesses^{11,12}

$$q\bar{q} \rightarrow t\bar{t}, \quad gg \rightarrow t\bar{t}, \quad (2.1)$$

as well as $O(\alpha_s^3)$ contributions.¹³ The cross sections for heavy-top-quark production have been presented in a number of works (see, e.g., Refs. 5, 6, and 11–15). However, the crucial cross sections are those which involve certain selection criteria. At the Tevatron ($\sqrt{S} = 2$ TeV), the cross section of (2.1) for $m_t = 180$ GeV is about 3.7 pb before any kinematic cuts. We still have to include the branching ratio for observing

$$t\bar{t} \rightarrow W^+ W^- jj,$$

with

$$W^+ W^- \rightarrow e^\pm \nu jj \text{ or } \mu^\pm \nu jj, \quad (2.2)$$

where one W decays hadronically (e.g., $W^+ \rightarrow u\bar{d}$ or $c\bar{s}$), and another W decays leptonically (e.g., $W^- \rightarrow e^- \bar{\nu}_e$ or $\mu^- \bar{\nu}_\mu$). The resulting cross section is

$$3.7 \text{ pb} \times \frac{2}{9} \times \frac{6}{9} \times 2 = 1.1 \text{ pb}. \quad (2.3)$$

In order to reduce the severe background for this decay mode from the

$$p\bar{p} \rightarrow W^\pm (\rightarrow e^\pm \nu \text{ or } \mu^\pm \nu) + \text{jet} \quad (2.4)$$

events, one must impose some kinematic cuts, e.g., transverse momentum and rapidity cuts. The resulting ratio of this signal to the major background from the process

$$p\bar{p} \rightarrow W^\pm (\rightarrow e^\pm \nu \text{ or } \mu^\pm \nu) + \text{jets} (\geq 2) \quad (2.5)$$

is still big. The details depend on the kinematic cuts imposed in the analysis, but it is typically of the order of 1/50 (Ref. 6). Of course, one can do better by requiring a high- P_T lepton associated with three high- P_T jets. In this case, most of the signal will be retained for a 180-GeV top quark, but the $W+jet$ background will be down by about a factor of 5–10 for

$$p\bar{p} \rightarrow W^\pm (\rightarrow e^\pm \nu \text{ or } \mu^\pm \nu) + \text{jet} (\geq 3) \quad (2.6)$$

events. In principle, one can even try to observe one high- P_T lepton associated with four high- P_T jets, and then use the dynamic likelihood method¹⁶ to discriminate the signal from its backgrounds. In addition, one may use the b -tagging⁷ method to further improve the ratio of signal to background at the cost of an 11% efficiency for tagging each $b \rightarrow \mu^- \bar{\nu}_X$. Since this is not the goal of this

work, we shall not pursue it any further. Instead, we shall discuss the “gold-plated” mode

$$W^+ W^- \rightarrow \mu^+ e^- \bar{\nu}_e \nu_\mu \text{ or } \mu^- e^+ \nu_e \bar{\nu}_\mu. \quad (2.7)$$

Its branching ratio is

$$\frac{1}{9} \times \frac{1}{9} \times 2, \quad (2.8)$$

which is $\frac{1}{12}$ of the decay mode (2.2). This yields about nine signal events at the upgraded Tevatron, before any cuts. For this small sample of signal events, the background from the continuum $W^+ W^-$ production and the $Z(\rightarrow \tau^+ \tau^-) + \text{jet} (\geq 0)$ processes should also be considered. Although it is not impossible to detect a 180-GeV top quark through this mode, it is definitely non-trivial. The inclusion of the $e^+ e^- \bar{\nu}_\nu$ and $\mu^+ \mu^- \bar{\nu}_\nu$ modes increases the signal by a factor of 2. But then additional sets of backgrounds⁶ should be considered, e.g., Drell-Yan, $b\bar{b}$ (including the flavor excitation), and muon punchthrough.

The determination of the top-quark mass from the process (2.1) will be difficult, either via the lepton + jets, or via the pure leptonic final states of that process.

Is there any process which can allow us to determine the top-quark mass more easily? The answer is yes, but more than one year of running at the upgraded Tevatron is needed (integrated luminosity of 100 pb⁻¹). We find that the W -gluon fusion process can provide the information on the top-quark mass more directly, provided the top quark is heavier than the W boson. Through the algorithm we shall introduce in the following sections, we find that an almost perfect efficiency for the “kinematic b tagging” and the determination of the longitudinal component of the neutrino momentum (both by kinematic methods) give us accurate information about the top-quark mass.

In the next section, we shall present the details of this new method, of detecting a heavy top quark at the upgraded Tevatron via the W -gluon fusion process.

III. HEAVY-TOP-QUARK PRODUCTION VIA W -GLUON FUSION

In this section we would like to discuss how to detect a 180-GeV top quark via the W -gluon fusion process

$$qg(W^+g) \rightarrow t\bar{b}q, \quad (3.1)$$

as shown in Fig. 1. Its cross section has been given in Refs. 17 and 18. However, it has not been discussed before how to detect a heavy quark using this process. It is the goal of this work.

The diagrams shown in Fig. 1 form a complete set of Feynman diagrams. They do not interfere with the Drell-Yan process¹⁸

$$qg \rightarrow q t \bar{b}. \quad (3.2)$$

The reason is that the $t\bar{b}$ pair in the W -gluon fusion process (3.1) is in a color-octet state, while the $t\bar{b}$ pair in the process (3.2) forms a color singlet. Also, the constituent cross section of (3.1) differs depending on whether the W boson is emitted from an initial quark or antiquark state.

The simplest way of computing this cross section would be to use the effective- W method.^{17,19} However, it is not well suited to our purpose because it neglects the P_T behavior of the scattered spectator quark. The transverse momentum P_T and rapidity Y behavior of the scattered quark will be the very tools we will use to discriminate this signal from its backgrounds. To make the text self-contained, we give the various relevant cross sections in Fig. 2 for the Tevatron. We use set 1 ($\Lambda=200$ MeV) of the parton distribution functions of EHLQ (Ref. 20), and evaluate them at $Q^2=M_W^2$ for the initial quark (antiquark) q which emitted the W boson, and at $Q^2=(m_t+m_b)^2$ for the gluon in the W -gluon fusion process (3.1). The cross sections of the processes (2.1) are evaluated for Q being the average value of the transverse masses of the outgoing primary particles, $M_T=(P_T^2+m^2)^{1/2}$. We take $m_b=5$ GeV, $M_W=81$ GeV, $M_Z=92$ GeV, and $\alpha=\frac{1}{128}$. The weak mixing angle is defined by $\cos\theta_W=M_W/M_Z$. The results are shown in Fig. 2 for the Tevatron ($\sqrt{S}=2$ TeV) as a function of the top-quark mass m_t . Only the lowest-order QCD subprocesses (2.1) are considered.

We have used $\sqrt{S}=2$ TeV instead of 1.8 TeV for the Tevatron because the signal event rate from process (3.1) gains about a factor of 1.4 for a larger proton-antiproton center-of-mass energy. For instance, the cross section of the process (3.1) with $m_t=180$ GeV and $m_b=5$ GeV is about 1.0 pb for $\sqrt{S}=2$ TeV, and 0.7 pb for $\sqrt{S}=1.8$ TeV.

For a 100-GeV top quark, the cross section of the QCD processes (2.1) is about 83 pb, and the W -gluon fusion (3.1) is about 9.8 pb (including both charges). But for a 180-GeV top quark, the cross section of the QCD

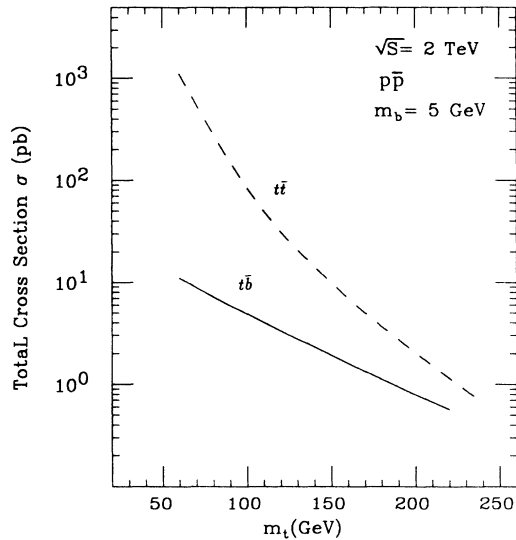


FIG. 2. The dashed line is the total $t\bar{t}$ production cross section vs m_t at a $p\bar{p}$ collider with $\sqrt{S}=2$ TeV. The solid line is the cross section of the $t\bar{b}$ production via W^+ -gluon fusion process, only one charged state is included. A factor of ~ 2 should be multiplied to include both $t\bar{b}$ and $\bar{t}b$ productions. m_b is the bottom-quark mass.

processes (2.1) is about 3.7 pb, and the W -gluon fusion (3.1) is about 2.0 pb (including both charges). These two processes only differ by a factor of 1.9 for $m_t=180$ GeV, instead of 8.5 in the $m_t=100$ GeV case.

As shown in Fig. 2, the cross section of $p\bar{p}(W^+g)\rightarrow t\bar{b}X$ is about 1.0 at $m_t=180$ GeV. Including both charges, we have 2.0 pb for the process $p\bar{p}(W^\pm g)\rightarrow t\bar{b}X$ or $\bar{t}bX$. The branching ratio for observing both the $e^+\nu_e b$ and $\mu^+\nu_\mu b$ modes of a top quark is about $\frac{1}{9}\times 2=\frac{2}{9}$. Hence, the event rate of observing t or \bar{t} via the decay modes of $e^\pm\nu_j$ or $\mu^\pm\nu_j$ is

$$(100 \text{ pb}^{-1})\times(2.0 \text{ pb})\times\frac{2}{9}=44 \text{ events} \quad (3.3)$$

before any kinematic cuts.

At first sight, this may not seem more advantageous than the detection of $t\bar{t}$ from the QCD processes (2.1) discussed in Sec. II. Recall that before any kinematic cuts we have about 110 signal events of (2.1) for semileptonic decay of one top quark and hadronic decay of another 9 signal events for the $e^\pm\mu^\mp$ mode, and 18 signal events if we include all the charged modes e^+e^- , $e^\pm\mu^\mp$, and $\mu^+\mu^-$. Keep in mind that all the above available channels may suffer completely different sets of backgrounds.

The method of detecting a heavy top quark via the process (3.1) is obviously different from that via the process (2.1). To emphasize these differences, we show in Fig. 3 the diagrams of the possible final states seen by the detector for the signal of one high- P_T lepton associated with jet(s). In Fig. 3(a), for the process (2.1), it is characterized by one high- P_T positron e^+ , missing E_T , and possibly 2, 3, or 4 hard jets, for $m_t=180$ GeV. In Fig. 3(b), for the process (3.1), it is characterized by one high- P_T positron e^+ , missing E_T , and typically 2 or 3 hard jets, again for $m_t=180$ GeV.

For the process (3.1), in Fig. 1, the propagator of the

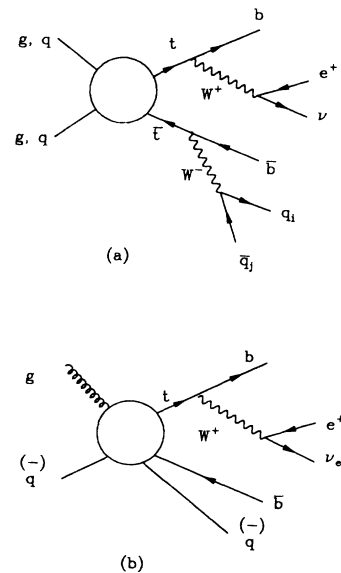


FIG. 3. (a) Shows the final states of the QCD process (2.1). (b) Shows the final states of the W^+ -gluon fusion process (3.1).

virtual W is roughly

$$\frac{1}{P_T^2 + M_W^2}, \quad (3.4)$$

where P_T is the transverse momentum of the W relative to the incident quark direction. The transverse momentum of the W -gluon (or $t\bar{b}$) system should be balanced by that of the jet formed by the spectator quark that emitted the virtual W . This raises the possibility of using the spectator quark to tag²¹ the W -gluon fusion process, Fig. 3(b).

At the pp collider SSC ($\sqrt{S} = 40$ TeV and integrated luminosity 10^7 nb⁻¹), this jet-tagging method will be extremely useful because the rapidity distribution, shown in Fig. 4, of this spectator quark from the W -gluon fusion process is very different from that of the usual QCD jet, which tends to peak at zero rapidity. Therefore, one can “kinematically tag” this quark jet to isolate the $t\bar{b}$ (or $t\bar{b}$) events produced via the W -gluon fusion mechanism from the electroweak-QCD background $W^\pm + \text{jet}(s)$. At the Tevatron collider, the available x value $[(\hat{S})^{1/2} = \sqrt{x_1 x_2 S}]$ is not as small as that at the SSC for the same heavy-quark mass. Hence, the spectator quark rapidity distribution peaks at a smaller $|Y|$, ~ 1.6 , shown in Fig. 5. Recall that at the SSC the rapidity distribution of the spectator quark peaks at $|Y| \sim 4$, shown in Fig. 4.

Furthermore, the spectator quark rapidity distribution is asymmetric in a $p\bar{p}$ collider if only one sign of lepton charge (e^+) is considered. This is due to the asymmetry of the relevant parton distributions of proton and antiproton. Provided the sign of the lepton charge can be measured,²² this rapidity asymmetry might provide a tool to confirm whether a top-quark signal at a $p\bar{p}$ collider indeed comes from the W -gluon fusion process. At the Tevatron, the spectator-quark rapidity distribution indeed shows an asymmetric behavior, as shown in Fig.

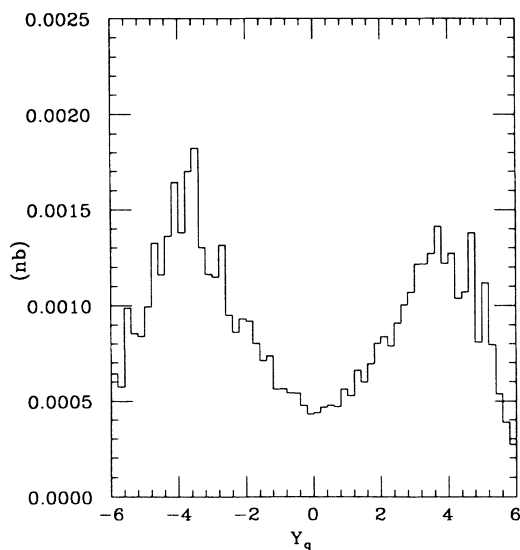


FIG. 4. The rapidity distribution of the spectator quark q in Fig. 3(b) for the W^\pm -gluon fusion process at the SSC collider ($\sqrt{S} = 40$ TeV).

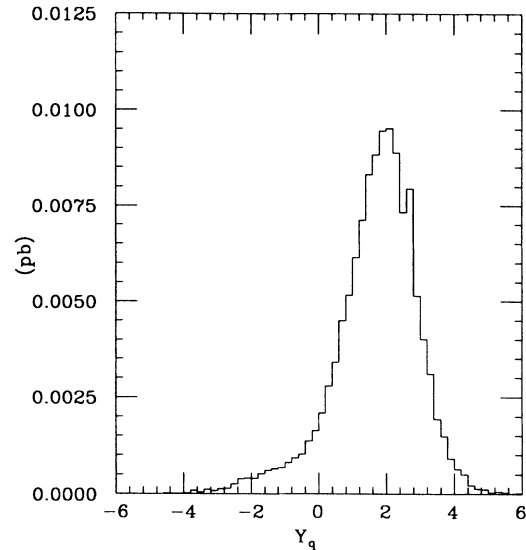


FIG. 5. The rapidity distribution of the spectator quark q in Fig. 3(b) for the W^+ -gluon fusion process at the Tevatron with $\sqrt{S} = 2$ TeV. Notice that only the positive charge state W^+ is considered.

5, in contrast with the peak at $Y=0$ for the usual QCD jet.

Because we would like to retain as many signal events as we can, we shall not make a tighter cut on this characteristic spectator-quark rapidity distribution. However, we shall use the unique characteristics associated with the W -gluon fusion mechanism to isolate this top-quark signal from its backgrounds. The details of this technique shall be presented in the following sections. Before we conclude this section we point out that the average P_T of the spectator quark is about $M_W/2$. This high P_T and the unique rapidity distribution of the spectator quark make it possible for us to kinematically tag the b quark, in Fig. 3(b), coming from the decay of the top quark produced via the W -gluon fusion process. Therefore, we can reconstruct the top-quark mass [the invariant mass of e^+ , ν_e , and b in Fig. 3(b)] without paying the price of a combinatorial factor to decide which is the “correct” b -quark jet among the typical 2 or 3 jets, as shown in Fig. 3(b).

IV. HEAVY-TOP-QUARK DETECTION AT THE TEVATRON

In this section, we present the results of some exercises using a parton-level Monte Carlo program²³ to study heavy-top-quark production from the W -gluon fusion process. We shall only consider the positive-charged channel, i.e., $t\bar{b}$ production, for the signal with top-quark mass $m_t = 180$ GeV at the upgraded Tevatron ($\sqrt{S} = 2$ TeV and integrated luminosity of 100 pb⁻¹). Only the decay mode

$$t \rightarrow bW^+ (\rightarrow e^+ \nu_e) \quad (4.1)$$

will be considered when we give our event rate. *In practice, it may be multiplied by 4 to account for both charged*

channels and the ability to detect muons. No attempt is made to simulate an actual detector when we consider our top-quark signal from the W -gluon fusion process. There is a very large background coming from

$$W^+(\rightarrow e^+\nu_e) + \text{jets } (\geq 2). \quad (4.2)$$

In principle, when we discuss the detection of a heavy-top quark via the W -gluon fusion process (3.1), we should consider top-quark production via the QCD process (2.1) as one of the backgrounds. However, because of the very different topological structures of these two kinds of events at the parton level, as discussed in the previous section, one can simply ignore the “background” from the QCD process (2.1). (We have checked that this contribution to the background is less than 1%.)

In Sec. IV A we discuss the signal. We discuss the $W^+ + \text{jet}$ background in Sec. IV B and give our conclusions for detecting a 180-GeV top quark at the upgraded Tevatron.

A. The heavy-top-quark signal from the W -gluon fusion process

As discussed in Sec. III the spectator quark q in Fig. 3(b) has a typical transverse momentum $P_T \simeq M_W/2$. For a 180-GeV top quark, the top quark will decay to a bottom quark b and a real W^+ boson. Both b quark and W^+ boson have the average P_T about $m_t/2\sqrt{2} \simeq 64$ GeV. However, the \bar{b} quark in Fig. 3(b) has a relatively low P_T . This gives us a convenient handle to “kinematically tag” the b quark from the P_T distribution, i.e., *the lowest- P_T jet among these three jets in Fig. 3(b) is unlikely to be the b -quark jet.* To distinguish the b quark from the q quark in Fig. 3(b), we shall use the characteristic rapidity distribution of the q quark, which is uniquely different in shape from the usual QCD jets, e.g., the b -quark jet, shown in

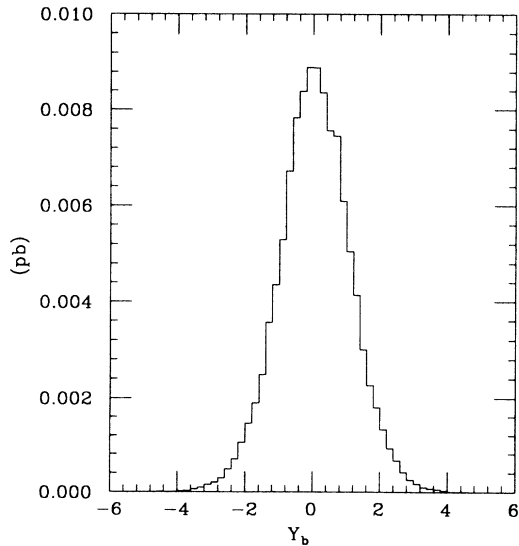


FIG. 6. The rapidity distribution of the b quark, in Fig. 3(b), for the W^+ -gluon fusion process at the Tevatron with $\sqrt{S} = 2$ TeV.

Fig. 6. For completeness, we also show the rapidity distribution of e^+ from the top-quark decay in Fig. 7. We then use the following algorithm to “kinematically tag” the b -quark jet in Fig. 3(b). First, find the two high- P_T jets, j_1 and j_2 . Then compare the absolute value of the rapidity $|Y|$ of j_1 and j_2 , and demand the one with the larger $|Y|$ to be the q -quark jet (we shall name this jet as j_1). The other one is the b -quark jet (called j_2 in the rest of this paper) decay from the top quark. The kinematic cuts for the following analysis are

$$\begin{aligned} P_T^{j_1} > 20, \quad P_T^{j_2} > 40, \quad P_T^{j_3} > 10, \quad E^{j_1} > 50, \\ P_T^e > 15, \quad E_T^{\text{missing}} > 15, \\ \Delta R(j_1, j_2) > 0.7, \quad \Delta R(j_1, j_3) > 0.7, \\ \Delta R(j_2, j_3) > 0.7, \\ |Y_{\text{jet}}| < 3.0, \quad |Y_e| < 1.5. \end{aligned} \quad (4.3)$$

Once we tag the b -quark jet (j_2) we can then reconstruct the transverse mass²⁴ of the decay products of the t quark, i.e., b , e^+ , and ν_e . The transverse mass M_T^{evb} is defined as

$$\begin{aligned} M_T^{evb} = & \{ [(E^b + E^e)^2 - (P_z^b + P_z^e)^2]^{1/2} \\ & + [(P_x^{\nu})^2 + (P_y^{\nu})^2]^{1/2} \}^2 \\ & - [(P_x^e + P_x^{\nu} + P_x^b)^2 + (P_y^e + P_y^{\nu} + P_y^b)^2]^{1/2}, \end{aligned} \quad (4.4)$$

where the missing E_T information has been used in this definition. We expect the distribution of the transverse mass M_T^{evb} peaks at the top-quark mass, as shown in Fig. 8. The tails on both sides of the peak are due in part to the probability of tagging the “wrong” b quark. The nonvanishing top-quark transverse momentum also contributes to the tails.²⁵ To select a sample to determine the top-quark mass from the invariant mass of e^+ , ν_e , and b , we impose a transverse-mass cut

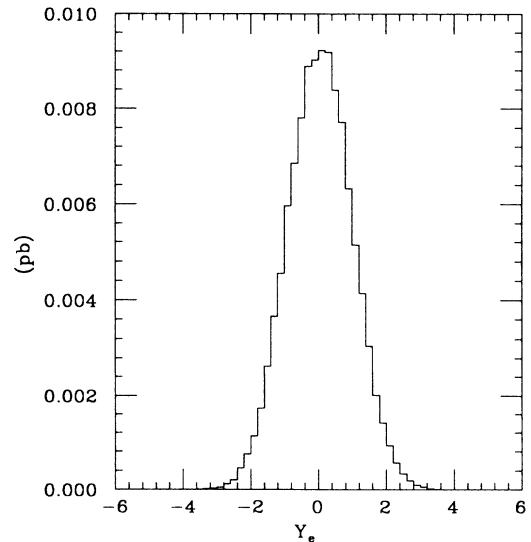


FIG. 7. The rapidity distribution of e^+ from a top-quark decay for the process (3.1) at the Tevatron with $\sqrt{S} = 2$ TeV.

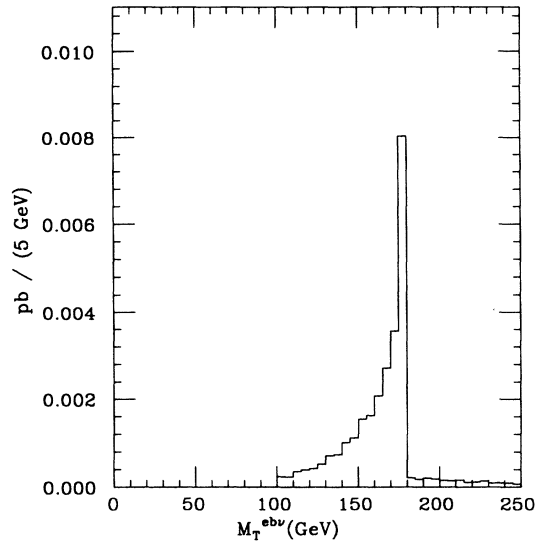


FIG. 8. The transverse-mass $M_T^{e\nu b}$ distribution for the process (3.1) at the Tevatron with $\sqrt{S} = 2$ TeV.

$$M_T^{e\nu b} > 100 \text{ GeV} \quad (4.5)$$

for $m_t = 180$ GeV. Since both e^+ and ν_e come from a real W^+ boson, we can use the W -boson mass constraint

$$M_W^2 = (p_e + p_\nu)^2 \quad (4.6)$$

to specify the longitudinal momentum P_z^ν of the neutrino. There are two solutions for P_z^ν , and most times both of them are physical solutions for a signal event. Therefore, one has to fix a prescription²⁶ to choose the one which will most likely give the correct distribution of the invariant mass of e^+ , ν_e , and b . We shall choose the one solution which has the smaller $|P_z^\nu|$.

We then construct the top-quark mass by

$$m_t^2 = (p_b + p_e + p_\nu)^2. \quad (4.7)$$

This is the unique handle for the W -gluon fusion process to determine the top-quark mass. Recall that in the process (2.1), it is nontrivial to reconstruct the top-quark mass, e.g., three-jet invariant mass M_{3j} (Ref. 6) due to the combinatorial factor of picking up the right three jets coming from the same top quark (or antiquark).

The result of the reconstructed top-quark invariant-mass distribution for the W -gluon fusion process is shown in Fig. 9. There are 2.8 signal events retained after all the above kinematic cuts. (This should be multiplied by four to account for both charged channels and the ability to detect muons.) This corresponds to a reduction of $2.8/11 = 0.25$ of the signal event rate. It has a very sharp peak within the 5-GeV-wide bin centered at the top-quark mass of 180 GeV. [The decay width of $\Gamma(t \rightarrow bW^+)$ is about 1.7 GeV for $m_t = 180$ GeV.] We find that this sharp peak indeed shows up in the invariant mass $M^{e\nu b}$ plot, Fig. 10, including both the signal (3.1) and background (4.9) events. [Only one charged mode (4.1) is included here.]

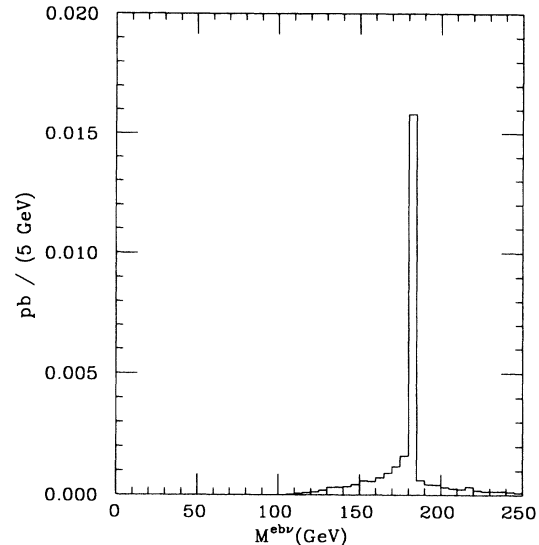


FIG. 9. The invariant-mass $M^{e\nu b}$ distribution for the process (3.1) at the Tevatron with $\sqrt{S} = 2$ TeV.

We emphasize that the above analysis algorithm has used both the transverse momentum P_T and the rapidity Y distribution of the spectator quark which emitted the virtual W in Fig. 1 to “kinematically tag” the b quark coming from the top-quark decay. Its efficiency is almost 100%. Furthermore, because there is only one neutrino involved in a signal event, we can easily reconstruct the top-quark mass by choosing the appropriate longitudinal momentum P_z^ν of the neutrino from the W -boson mass constraint (4.6). In the next subsection, we will find that the “kinematic b -tagging” algorithm is a useful tool to

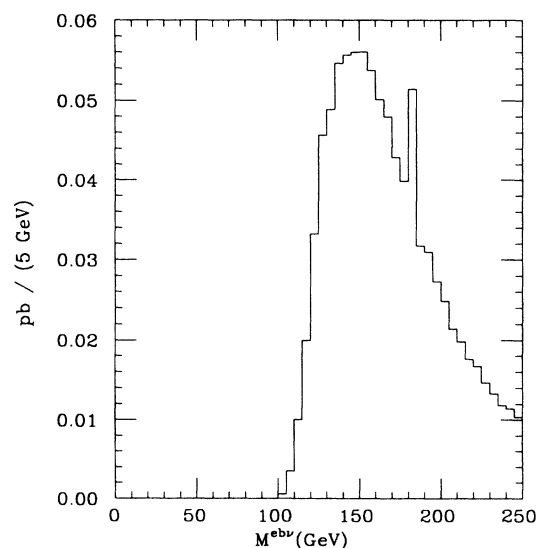


FIG. 10. The invariant-mass $M^{e\nu b}$ distribution for the sum of the signal (4.8) and the background (4.9) events after the cuts (4.3) and (4.5) at the Tevatron with $\sqrt{S} = 2$ TeV. Only one charged mode (4.1) is included here.

discriminate a top-quark signal from its W +jet backgrounds

B. W +jet background

The major background for detecting the top-quark signal via the process (3.1) for $m_t=180$ GeV is the $W^++\text{jet}(\geq 2)$ processes. It turns out that the W^++2 jet background is too big to detect the top-quark signal via the W -gluon fusion process for $m_t=180$ GeV at the upgraded Tevatron (more discussions related to the W^++2 jet background can be found in the Appendix). Hence, we should study the W^++3 jet process consistent with what was discussed in the previous section for the signal process (3.1). After imposing the same set of kinematic cuts, as shown in Eq. (4.3), we obtain about 2.8 signal events and 100 background events. Although the ratio of signal to background is small, $\sim \frac{1}{36}$, the total background event number is not the issue in detecting the top quark via the process (3.1). The relevant quantity is the invariant mass M^{evb} distribution in Fig. 10. Therefore, if one can do the mass resolution M^{evb} up to the accuracy of 5 GeV or better, then the sharp peak in Fig. 10 will show the top-quark signal distinctly over the W^++3 jet background. The top-quark mass is therefore determined.

More than half of the total signal events are retained within the 5-GeV-wide bin containing the peak. This corresponds to 1.6 signal events of

$$\begin{aligned} qg(W^+g) &\rightarrow t\bar{b}q \\ &\rightarrow W^+b\bar{b}q \\ &\rightarrow e^+\nu_e b\bar{b}q. \end{aligned} \quad (4.8)$$

Within the same bin, we have about 3.8 background event of

$$W^+(\rightarrow e^+\nu_e)+3 \text{ jets}. \quad (4.9)$$

If we include both charged states (W^\pm) and assume we can detect muons as well, then, within the same bin, the ratio of signal to background

$$\frac{S}{B} \simeq \frac{6.5}{15} = 0.43. \quad (4.10)$$

The significance of the signal to background is therefore

$$\frac{S}{\sqrt{B}} = \frac{6.5}{\sqrt{15}} \simeq 1.7. \quad (4.11)$$

One may gain an even better S/B by applying the charged-particle multiplicity cut²⁷ at the cost of some signal events. We shall not apply those cuts in our study here. Because of the small number of signal events, more than one year of running is needed at the upgraded Tevatron with integrated luminosity of 100 pb^{-1} .

For a second-phase upgraded Tevatron ($\sqrt{S}=2$ TeV and integrated luminosity of 500 pb^{-1}), the significance of the signal to background is

$$\frac{S}{\sqrt{B}} = \frac{33}{\sqrt{75}} \simeq 3.8.$$

We conclude that a heavy top quark with mass 180 GeV can be detected provided the mass resolution of M^{evb} can be done with an accuracy of 5 GeV or better.

Before we leave this section, we point out that the $W+3$ jet background given above is evaluated at $Q^2=\hat{S}$. We have checked other Q^2 choices, and the cross section can differ by a factor of 2 in our analysis. The cross section we presented here is the most conservative one. In addition, the shape of the M^{evb} distribution from the $W+3$ jet process varies with different choice of Q^2 .

Furthermore, the event numbers given in this paper can be expected to degrade when realistic detector effects are included, but they illustrate the fact that the W -gluon fusion process (3.1) can be a useful process for detecting a heavy top quark. It can also be a useful process for detecting possible sequential-generation quarks. In that case, one should further consider the reduction in the cross section due to either the flavor-mixing angle or the production of a pair of heavy quarks, e.g., t' and b' .

In the next section, we shall turn from the Tevatron to the SSC.

V. HEAVY-TOP-QUARK DETECTION AT THE SSC

In previous sections, we have learned that the W -gluon fusion process

$$qg(W^+g) \rightarrow t\bar{b}q$$

can be very useful to detect a heavy top quark or a possible fourth-generation quark at the Tevatron. Because this process becomes more important when the quark becomes more massive, as shown in Fig. 11, we should study a heavy-quark production via this process at the SSC ($\sqrt{S}=40$ TeV and integrated luminosity 10^4 pb^{-1}).

This section is devoted to the detection of a 180-GeV top quark at the SSC via the W -gluon fusion process (3.1). The analysis procedures are exactly the same as those discussed in the previous section. We shall again use the

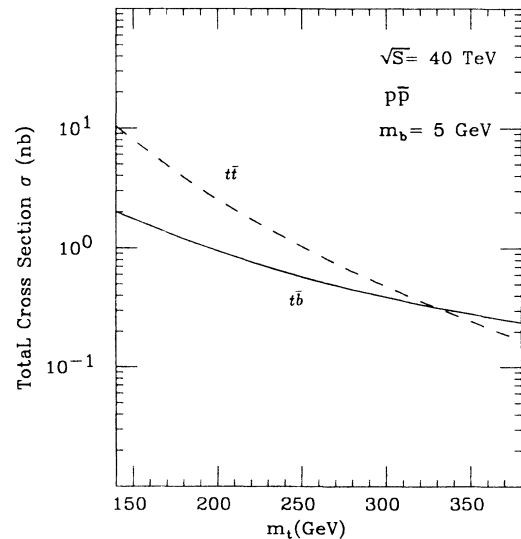


FIG. 11. Same as Fig. 2, but for the SSC collider.

use the unique characteristics of the P_T and Y distributions of the spectator quark q in process (3.1) to discriminate the signal from its background. However, the rapidity Y distribution of this spectator quark, shown in Fig. 4, is no longer asymmetric because this is a proton-proton collider.

We found that at the SSC the signature

$$qg(W^+g) \rightarrow W^+(\rightarrow e^+\nu) + 2 \text{ jets} \quad (5.1)$$

of the signal (3.1) is already large enough to give a sharp peak in the top-quark invariant-mass M^{evb} plot, as shown in Fig. 12, including both the signal (3.1) and the electroweak-QCD background. Hence we shall study the top-quark (via the W -gluon fusion mechanism) signature characterized by one high- P_T positron e^+ , missing E_T , and two hard jets, at the SSC.

The electroweak-QCD background

$$W^+(\rightarrow e^+\nu) + 2 \text{ jets} \quad (5.2)$$

is obtained using the parton-level Monte Carlo program PAPAGENO, which has the exact $2 \rightarrow 3$ matrix element for this process. In the kinematic region, Eq. (5.3), relevant to our study here, there is no infrared or collinear divergences coming from the PAPAGENO Monte Carlo program.

The kinematic cuts we imposed for the study of a 180-GeV top quark are

$$\begin{aligned} P_T^{j_1} > 40, \quad P_T^{j_2} > 40, \quad P_T^e > 20, \quad E_T^{\text{missing}} > 20, \\ \Delta R(j_1, j_2) > 0.7 \quad |Y_{\text{jet}}| < 5.0, \quad |Y_e| < 2.0. \end{aligned} \quad (5.3)$$

To select a sample for determining the top-quark mass from the invariant mass M^{evb} , we impose a transverse-mass cut

$$M_T^{evb} > 140 \text{ GeV} \quad (5.4)$$

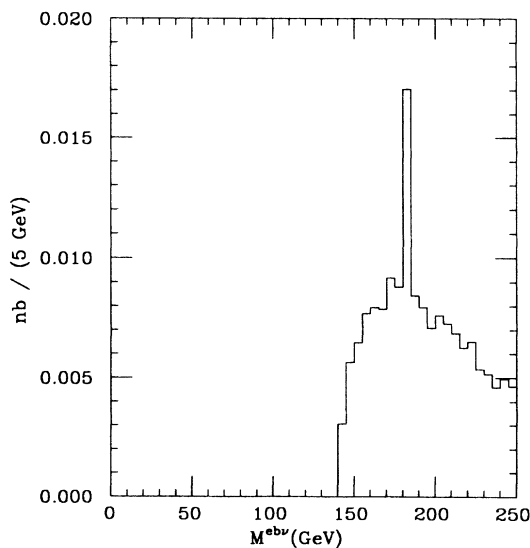


FIG. 12. The invariant-mass M^{evb} distribution for the sum of this signal (5.1) and the background (5.2) events after the cuts (5.3) and (5.4) at the SSC with $\sqrt{S} = 40$ TeV. Only one charged mode (4.1) is included here.

for $m_t = 180$ GeV. The resulting M^{evb} distribution is shown in Fig. 12. There are 2.4×10^5 signal events of (5.1) and 3.2×10^6 background events of (5.2) retained after the kinematic cuts (5.3). This gives about 2.1×10^5 signal events and 2.5×10^6 background events after the transverse-mass cut (5.4). Including both charged states and assuming the ability to detect muons, within a 5-GeV-wide bin around 180 GeV of M^{evb} , for $m_t = 180$ GeV, we have about

$$\frac{S}{B} = \frac{38 \times 10^4}{31 \times 10^4} = 1.2, \quad \frac{S}{\sqrt{B}} = 680. \quad (5.5)$$

The high signal event rate yields a 680σ effect. Therefore, we conclude that the W -gluon fusion process (3.1) is most useful in detecting a heavy top quark with mass $m_t = 180$ GeV at the SSC.

A similar procedure can be applied for detecting a possible fourth-generation quark at the SSC. We shall leave this for a future study.

VI. CONCLUSION

On the basis of the unique transverse momentum P_T and rapidity Y distributions of the spectator quark which emitted the W -boson for W -gluon fusion which produces a heavy top quark, we conclude that the W -gluon fusion process is most useful for detecting a heavy top quark at the upgraded Tevatron with $\sqrt{S} = 2$ TeV and integrated luminosity 100 pb^{-1} . In this paper, we have focused on the example of a 180-GeV top quark and conclude that a 5-GeV mass resolution of M^{evb} would be desired at the upgraded Tevatron for its detection. Also, more than one year of integrated luminosity is needed. To gain a factor of 1.4 in the signal event rate at the upgraded Tevatron, we prefer its center-of-mass energy to be $\sqrt{S} = 2$ TeV, instead of 1.8 TeV. In addition, we showed that the W -gluon fusion becomes more important for more massive quarks (either a top quark or a possible fourth-generation quark). At the upgraded Tevatron, one might not have enough signal events to detect a more massive top quark, say, 200 GeV, in one Tevatron year. However, at the SSC, one can explore a more extensive range of the heavy-quark mass.

Through similar analysis procedures, we also showed that the W -gluon fusion process is most useful in detecting a heavy quark at the SSC. The large event rate of the signal yields a large significance for detecting a heavy quark at the SSC.

Because we can “kinematically tag” the b quark in the signal process of Fig. 3(b) using the unique features of the P_T and Y distributions of the spectator quark q , and determine the longitudinal moment P_z^y of the neutrino by choosing the smaller $|P_z^y|$ of the two solutions from the W -boson mass constraint, Eq. (4.6), we can determine the top-quark mass “precisely,” provided a 5-GeV (or better) mass resolution of M^{evb} can be achieved at the upgraded Tevatron. Presumably, because of the high signal event rate, a less accurate measurement of the invariant mass M^{evb} is allowed for detecting a 180-GeV top quark at the SSC.

We have chosen a 180-GeV top quark as our example

to perform a Monte Carlo study at both the upgraded Tevatron and SSC, and conclude that the W -gluon fusion mechanism is most useful to detect a 180-GeV top quark. The same conclusion should hold for any top quark with $m_t > M_W$. Recall that at the upgraded Tevatron, a 180-GeV top-quark event rate from the QCD process (2.1) is only about a factor of 1.9 larger than that from the W -gluon fusion process (3.1). At SSC, this factor is about 3.5. Hence the W -gluon fusion mechanism gets more important as the top-quark mass gets heavier, provided there are enough signal events retained to gain a reasonable significance of the signal-to-background ratio. For instance, this mechanism will work better for detecting a 140-GeV than 90-GeV top quark. There is a bigger chance for a heavier top quark to have at least two high P_T jets in the signal event in order to stand out against the electroweak QCD background $W + \text{jets} (\geq 2)$ in the invariant-mass $M^{e\nu b}$ plot. The details for various heavy-quark masses should be worked out through a Monte Carlo study, separately.

Finally, we emphasize that the “kinetic b -tagging” efficiency is almost 100%. The experimental detection efficiency is not included here. But one can gain a better S/B by applying, for instance, the charged-particle multiplicity cut at the cost of some signal events. For the W -gluon fusion process we emphasize again the characteristic features of the P_T and Y distributions of the spectator quark which emitted the virtual W . This is unique in the W -gluon fusion process (3.1), unlike the usual QCD process (2.1), where one has to pay a 89% reduction of the signal rate for tagging each $b \rightarrow \mu^- \bar{\nu}_X$. The consequence of this “kinematic b tagging” in the W -gluon fusion process is the ability to reconstruct the invariant mass $M^{e\nu b}$ and, hence, determine the top-quark mass via the process (3.1). This feature is absent in the usual QCD process (2.1). There, one has to overcome the combinatorial factor for kinematically tagging the right b quark associated with the lepton to reconstruct the top-quark transverse mass $M_T^{e\nu b}$ or the three-jet invariant mass M_{3j} if the lepton + 4 jet mode is under study. For the dilepton mode of $t\bar{t}$ events, since there are two neutrinos involved in the such events, it will be very difficult to reconstruct the top-quark mass.

Therefore, we conclude that the W -gluon fusion process can be useful in detecting a heavy quark at both the upgraded Tevatron and SSC. In principle, the same conclusion should also hold for the pp collider LHC; we leave this for a future study.

ACKNOWLEDGMENTS

The author would like to thank G. L. Kane, Y.-P. Yao, and K.-C. Wang for many stimulating discussions; and H. Baer and E. L. Berger for many useful conversations. Thanks are also due to the members of the Heavy Quarks Working Group of the CDF Collaboration Workshop at Fermilab in 1989, especially to P. Sinervo and J. Yoh. He also wishes to thank P. Arnold, E. Eichten, T. Han, S. Kuhlman, L. Nodulman, F. Paige, D. Sivers, W.-K. Tung, A. White, B. Wicklund, C. Zochos, and D. Zep-

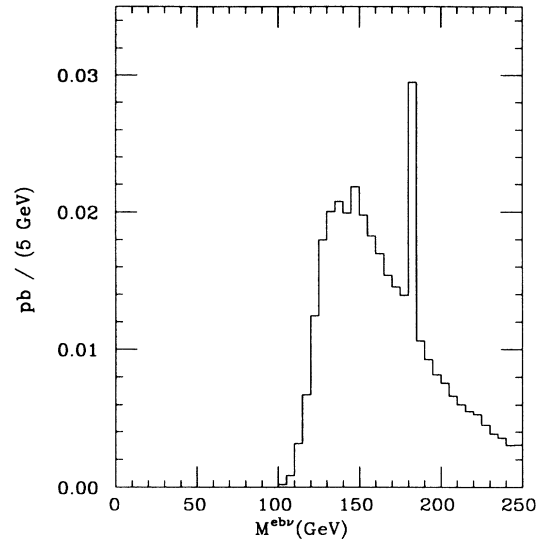


FIG. 13. The invariant-mass $M^{e\nu b}$ distribution for the sum of the signal (4.8) and the “pseudo $W^+ + 3$ jet background” (A1) events after the cuts (4.3) and (4.5) at the upgraded Tevatron with $\sqrt{S} = 2$ TeV. Only one charged mode (4.1) is included here.

penfeld for discussions. This work was supported in part by the U.S. Department of Energy, Division of High Energy Physics, Contract No. W-31-109-ENG-38.

APPENDIX

In Sec. IV we have discussed the $W + 3$ jet background events for detecting a 180-GeV top quark via the W -gluon fusion process at the upgraded Tevatron. In this appendix, we would like to estimate the $W^+ + 3$ jet background by naively multiplying a factor of $\alpha_s \sim \frac{1}{10}$ to the event rate of the $W^+ + 2$ jet process using the parton-level Monte Carlo program PAPAGENO (Ref. 10) which has the exact $2 \rightarrow 3$ matrix element for the $W^+ + 2$ jet process, and repeat the analysis done in Sec. IV for this “pseudo $W^+ + 3$ jet background”:

$$\frac{1}{10} \sigma(p\bar{p} \rightarrow W^+ (\rightarrow e^+ \nu_e) + 2 \text{ jets}) . \quad (\text{A1})$$

After imposing a subset of the kinematic cuts (4.3) and (4.5) without the j_3 constraints, we obtain about 33 events of this kind (a factor of $\frac{1}{10}$ has been included) of background (A1).

The resulting top-quark invariant mass $M^{e\nu b}$, including both the signal from the W^+ -gluon fusion process (3.1) and the background from the “pseudo $W^+ + 3$ jet” process (A1), is shown in Fig. 13.

If we include both charged states (W^\pm) and assume we can detect muons as well, then, within the 5-GeV-wide bin containing the peak, we have the ratio of signal to background

$$\frac{S}{B} \simeq \frac{6.5}{4.4} = 1.5 . \quad (\text{A2})$$

The significance of the signal to background is, therefore,

$$\frac{S}{\sqrt{B}} \simeq 3.1 . \quad (\text{A3})$$

Comparing (A2) with (4.10), we found that the $W + 3$ jet background is only a factor of 2.9 smaller than the $W + 2$ jet background. This is a factor of 3.4 bigger than the naive α_s argument.

- ¹CLEO Collaboration, A. Bean *et al.*, Phys. Rev. D **35**, 3533 (1987); JADE Collaboration, W. Bartel *et al.*, Phys. Lett. **146B**, 437 (1984).
- ²V. Barger and S. Pakvasa, Phys. Lett. **81B**, 195 (1979); G. L. Kane and M. Peskin, Nucl. Phys. **B195**, 29 (1982); for a review see J. C. Taylor, *Gauge Theories of Weak Interactions* (Cambridge University Press, Cambridge, England, 1976).
- ³P. Sinervo, in Proceedings of the Second International Symposium on the Fourth Family of Quarks and Leptons, Santa Monica, California, 1989 (unpublished).
- ⁴U. Amaldi *et al.*, Phys. Rev. D **36**, 1385 (1987); G. Costa *et al.*, Nucl. Phys. **B297**, 244 (1988); J. Ellis and G. Fogli, Phys. Lett. B **213**, 526 (1988).
- ⁵H. Baer, V. Barger, H. Goldberg, and R. J. N. Phillips, Phys. Rev. D **37**, 3125 (1988).
- ⁶J. L. Rosner, Phys. Rev. D **39**, 3297 (1989); H. Baer, V. Barger, and R. J. N. Phillips, *ibid.* **39**, 3310 (1989); R. Kleiss, A. D. Martin, and W. J. Stirling, Z. Phys. C **39**, 393 (1988); S. Gupta and D. P. Roy, Z. *ibid.* **39**, 417 (1988); F. Halzen, C. S. Kim, and A. D. Martin, Durham Report No. DTP/88/34 (unpublished).
- ⁷C. Habber, in *Proceedings of the Seventh Topical Workshop on Proton-Antiproton Collider Physics*, Batavia, Illinois, edited by R. Raja and J. Yoh (Fermilab, Batavia, 1988).
- ⁸G. L. Kane, J. Vidal, and C.-P. Yuan, Phys. Rev. D **39**, 2617 (1989).
- ⁹V. Barger, T. Han, J. Ohnemus and D. Zeppenfeld, Phys. Rev. D **40**, 2888 (1989).
- ¹⁰I. Hinchliffe, PAPAGENO version 2.76.
- ¹¹For a review, see E. L. Berger, in *Proceedings of the XXIV International Conference on High Energy Physics*, Munich, West Germany, 1988, edited by R. Kotthaus and J. H. Kuhn (Springer, Berlin, 1989), p. 987.
- ¹²B. L. Combridge, Nucl. Phys. **B151**, 429 (1979); K. Hagiwara and T. Yoshino, Phys. Lett. **80B**, 282 (1979); L. M. Jones and H. W. Wyld, Phys. Rev. D **17**, 1782 (1978); H. Georgi *et al.*, Ann. Phys. (N.Y.) **114**, 273 (1978); J. Babcock, D. Sivers, and S. Wolfram, Phys. Rev. D **18**, 162 (1978); E. L. Berger, *ibid.* **37**, 1810 (1988); V. Barger, H. Baer, K. Hagiwara, and R. J. N. Phillips, *ibid.* **30**, 947 (1984); J. L. Rosner, Phys. Lett. **146B**, 108 (1984); I. Bigi, Y. Dokshitzer, V. Khoze, J. Kuhn, and P. Zerwas, Phys. Lett. B **181**, 157 (1986); G. Pancheri, S. Geer, and Y. N. Srivastava, *ibid.* **192**, 223 (1987); P. Colas and D. Denegri, *ibid.* **195**, 295 (1987); H. Baer, V. Barger, and R.J.N. Phillips, Phys. Rev. D **39**, 2809 (1989).
- ¹³R. Kleiss and W. J. Stirling, Z. Phys. C **40**, 419 (1988); P. S. Dimitriadis, L. B. Papatsimps, and S. D. P. Vlassopoulos, Phys. Rev. D **38**, 2776 (1988); P. Nason, S. Dawson, and R. K. Ellis, Nucl. Phys. **B303**, 607 (1988); G. Altarelli, M. Diemoz, G. Martinelli, and P. Nason, *ibid.* **B308**, 724 (1988); A. D. Martin, W. J. Stirling, and R. G. Roberts, Z. Phys. C **42**, 277 (1989); R. K. Ellis, in *Proceedings of the Seventh Topical Workshop on Proton-Antiproton Collider Physics* (Ref. 7); P. Nason, ETH (Zurich) Reports Nos. ETH-PT/88-11 and 14, 1988 (unpublished); W. Beenakker, H. Kuijf, W. L. van Neerven, and J. Smith, University of Leiden/State University of New York (Stony Brook) report, 1988 (unpublished).
- ¹⁴E. L. Berger, D. Kuebel, F. Paige, M. Pundurs, and C.-P. Yuan (in preparation).
- ¹⁵A concise summary of some search techniques and further references may be found in R. J. N. Phillips, in *Proceedings of the XXIV International Conference on High Energy Physics* (Ref. 11).
- ¹⁶K. Kondo, J. Phys. Soc. Jpn. **57**, 4126 (1988).
- ¹⁷S. Dawson, Nucl. Phys. **B249**, 42 (1985); S. Dawson and S. S. D. Willenbrock, *ibid.* **284**, 449 (1987).
- ¹⁸S. S. D. Willenbrock and D. A. Dicus, Phys. Rev. D **34**, 155 (1986).
- ¹⁹W. Repko and Wu-Ki Tung, in *Physics of the Superconducting Super Collider, Snowmass, 1986*, proceedings of the Summer Study, Snowmass, Colorado, edited by R. Donaldson and J. Marx (Division of Particles and Fields of the APS, New York, 1987); S. Dawson, Nucl. Phys. **B249**, 42 (1985); G. L. Kane, W. Repko, and W. Rolnick, Phys. Lett. **148B**, 367 (1984); M. Chanowitz and M. K. Gaillard, *ibid.* **142B**, (1984); Nucl. Phys. **B261**, 379 (1985).
- ²⁰E. Eichten, I. Hinchliffe, K. Lane, and C. Quigg, Rev. Mod. Phys., **56**, 579 (1984).
- ²¹R. Kleiss and W. J. Stirling, Phys. Lett. B **200**, 193 (1988); R. N. Cahn, S. D. Ellis, R. Kleiss, and W. J. Stirling, Phys. Rev. D **35**, 1626 (1987).
- ²²We are grateful to H. Baer for this comment.
- ²³Written by the author.
- ²⁴E. L. Berger, D. Dibitonto, M. Jacob, and W. J. Stirling, Phys. Lett. **140B**, 259 (1984).
- ²⁵We are grateful to E. L. Berger for this comment.
- ²⁶G. L. Kane and C.-P. Yuan, Phys. Rev. D **40**, 2231 (1989); C.-P. Yuan, Ph.D. thesis, University of Michigan, 1988.
- ²⁷J. F. Gunion, G. L. Kane, C.-P. Yuan, H. F.-W. Sadrozinski, A. Seiden, and A. J. Weinstein, Report No. ANC-HEP-PR-89-34, 1989 (unpublished); H. F.-W. Sadrozinski, A. Seiden, and A. J. Weinstein, in *High Energy Physics in the 1990's*, Snowmass, Colorado, 1988, edited by S. Jensen (World Scientific, Singapore, 1989); C.-P. Yuan, Ph.D thesis, University of Michigan, 1988.